Structural and NMR properties of niobium dichalcogenides intercalated with post transition metals*

N. Karnezos and L. B. Welsh†
Department of Physics, Northwestern University, Evanston, Illinois 60201

M. W. Shafer
IBM T. J. Watson Research Center, Yorktown Heights, New York 10598

(Received 9 September 1974)

The intercalation phase of the transition-metal dichalcogenide $NbSe_2$, intercalated with Ga, In, Tl, Sn, and Pb, as well as NbS_2, intercalated with In, have been prepared and studied by a variety of techniques. For most intercalates, single-intercalation-phase samples of the formula $M_{2/3}NbX_2$ were obtained, where M is the intercalate and X a chalcogen. The changes in the lattice parameters occurring upon intercalation have been determined from x-ray powder patterns. No superconducting transition was observed in any of the intercalated samples above 1.5 K. The microscopic properties were studied from 1.5 to 4.2 K using nuclear-magnetic-resonance (NMR) techniques, with the prime emphasis on the determination of the electric field gradients (EFG) at the Nb sites. For each intercalated sample the EFG was reduced by (35–60)% from that found in NbS_2 and $NbSe_2$. For the $Tl_{2/3}NbSe_2$ sample, the Nb line shape was fit by a single EFG while for all other intercalates at least two EFGs were needed to fit the Nb line shape, indicating two sites with inequivalent NMR properties. This change in the EFG at the Nb sites upon intercalation is attributed to charge transfer from the intercalated atoms into the conduction band of the layered compound. Knight-shift and spin-lattice relaxation-time measurements on the intercalate resonance indicate conduction-band behavior at the intercalate site but with a low density of states at the Fermi energy. The Sn Mössbauer line shape was studied in $Sn_{2/3}NbSe_2$. Only a single resonance was observed indicating a lack of any large quadrupole splitting as opposed to the two-line spectrum which has been observed for Sn in Sn_1TaS_2.

INTRODUCTION

Recently, the structural, optical, and electronic properties of the transition-metal layered dichalcogenides have been studied extensively because of their highly anisotropic behavior. These compounds have the general formula TX_2, where T is a transition metal from the groups IVb, Vb, and VIb of the Periodic Table and X is one of the chalcogens, sulfur, selenium, or tellurium. Typically the TX_2 compounds with transition metals from groups IVb and VIb exhibit semiconducting or insulating properties, while those with transition metals from column Vb exhibit metallic and superconducting properties at low temperatures.

The structures of these layered compounds have been studied extensively and their physical properties have been reviewed by Wilson and Yoffe.[1] They can be described as two-dimensional X-T-X layers, with strong bonding between atoms in the same layer and relatively weak van der Waals type forces between atoms in different layers. Because of the weak interlayer bonding in these materials, electron-donor organic molecules[2–4] or metal atoms[5–8] can penetrate between the layers to form an intercalated complex with alternating layers of the TX_2 compound and the intercalate atoms or molecules. Owing to their two-dimensional character, these materials have strongly anisotropic bulk properties. For example, conductivity measurements[9] on the $2H$ polytype of $NbSe_2$ indicate an anisotropic electrical conductivity, with the conductivity along the layers being at least 10–30 times larger than that perpendicular to the layers. The critical field for superconductivity has also been found to be strongly anisotropic, and can be quite large when the field is applied parallel to the layers.

There have been a number of studies of the electronic and bulk properties of the group-Vb transition-metal layered compounds undertaken in order to understand the effect of intercalation on the electronic and structural properties of these materials. The materials which have been studied in detail are the intercalation compounds of TaS_2 and $NbSe_2$. The intercalation compounds of TaS_2 have received the most attention because of the ease with which a wide variety of atoms and molecules which act as electron donors may be intercalated. When a donor atom or molecule is intercalated there is a substantial charge transfer to the conduction bands (primarily the T d band) of the layered compound. Such a charge transfer will change the density of states at the Fermi energy. This is indicated by the specific-heat data on TaS_2 intercalated with pyridine[10] which shows an increase in the density of states over pure TaS_2. The superconducting transition temperature was also found to increase from 0.8 K for TaS_2 to 3.5 K for TaS_2 intercalated with pyridine. On the other hand,

intercalation with metal atoms has been found to either decrease or increase the superconducting transition temperature T_c, from that of the unintercalated material depending on the degree of intercalation. While these results suggest charge transfer is occurring, in the case of the TaS_2 intercalation compounds it has not been possible to determine the charge transfer directly on the basis of microscopic measurements such as nuclear magnetic resonance (NMR). (In the Ta compounds only, the intercalate resonance has been studied because of the very large quadrupole splitting of the Ta NMR.) The advantage of investigating the properties of the intercalated compounds of $NbSe_2$ or NbS_2, rather than those of TaS_2, are that the changes in the local electronic properties which occur at both the Nb and intercalate sites upon intercalation can be studied in favorable cases using NMR techniques.

In this study we report the results of structural studies and T_c, NMR, and Mössbauer-effect measurements on $NbSe_2$ and NbS_2 which have been intercalated with the group-IIIa and -IVa post transition metals Ga, In, Tl, Sn, and Pb. This is the first time that intercalation of these elements into $NbSe_2$ or NbS_2 has been reported. From the Nb NMR quadrupolar splitting we have determined the change in the electric field gradients (EFG) at the Nb sites occurring upon intercalation and estimated the charge transfer from the intercalate atoms to the Nb d band. In favorable cases the intercalate NMR Knight shift and spin-lattice relaxation time (T_1) have been measured. These results are compared with the results obtained by Gossard *et al.*[11] in the TaS_2 intercalated compounds. Finally, we discuss the results of Sn Mössbauer-effect measurements in the Sn intercalated compounds.

EXPERIMENTAL RESULTS

Sample preparation and structure

The NbS_2 and $NbSe_2$, which were used as the starting materials for the preparation of the intercalation compounds, were prepared by reacting the elements in sealed silica tubes. Several firings at (800–900) °C were necessary to produce powders of single-phase material having the $2H$-type structure. The intercalation of the metals was carried out by reacting the powdered niobium dichalcogenides with the metal vapor at (800–950) °C, in sealed silica tubes. The chalcogenide powders and the condensed metal phase were separated during the intercalation reaction so that it proceeded via the vapor rather than the liquid or solid metal phase. Only by repeated firing and subsequent grinding could reproducibly homogeneous materials be produced by this method. The composition, i.e., the value of x in M_xNbX_2, was determined by measuring the weight increase of the dichalcogenides. In selected cases complete elemental analyses were done by classical techniques to confirm the validity of the weight-gain method. All samples were x rayed using powder diffraction techniques to determine the number of phases present as well as their lattice parameters. These data are summarized in Table I. In general it seems the $2H$ polytype is maintained after intercalation, but in some cases the intercalated sample appeared to be disordered so the resulting patterns were broad and difficult to interpret. The x-ray powder patterns were checked again after the NMR spectra were obtained and no change was observed, indicating no substantial deterioration of the samples with either limited exposure to air or temperature recycling from room temperature to 4.2 K. The data indicate that the intralayer symmetry is unchanged and the bond lengths within a layer are only slightly increased by the metal intercalation. Thus the major structural change which occurs is the rather large separation of the layers to accommodate the metal atoms. We have not done any detailed structural studies to determine the exact position of the intercalated species but from other studies[5,7,8] and crystal chemical relationships we can assume an octahedral or distorted-octahedral-type environment. Figure 1(a) shows the tetrahedrally or octahedrally coordinated intercalate positions[5] (holes) for the case of $2H$-TaS_2 which has the same structure as $2H$-NbX_2. The increase of the lattice parameter in the c direction should be noted. For the single-phase materials, where Pb, Sn, and In are the intercalate, an increase of 6.0 Å is seen in all three cases. This is perhaps consistent with a model where these "metals" with radii somewhere between that of the pure metal and of a low-oxidation-state ion, are intercalated between every layer. For the Tl intercalated sample the c axis increases by only 4

TABLE I. Summary of compounds prepared with formula M_xNbX_2 where $x \approx \frac{2}{3}$. Also included are the c- and a-axis parameters of the hexagonal unit cell determined from x-ray powder patterns.

Material	Lattice parameters a(Å)	c(Å)	Comments
$Tl_{0.64}NbSe_2$	3.46	16.6	Single phase
$In_{0.62}NbSe_2$	3.47	18.6	Single phase
$Pb_{0.63}NbSe_2$	3.46	18.6	Single phase
$Sn_{0.61}NbSe_2$	3.48	18.6	Single phase
$Sn_{0.56}NbSe_2$	3.48	18.6	Contains 10% unknown phase
$Ga_{0.5-0.7}NbSe_2$	...	17.6	Contains three phases
$In_{0.68}NbS_2$	...	17.6	Broad x-ray lines, could contain another phase
$NbSe_2$	3.45	12.56	
NbS_2	3.34	11.91	

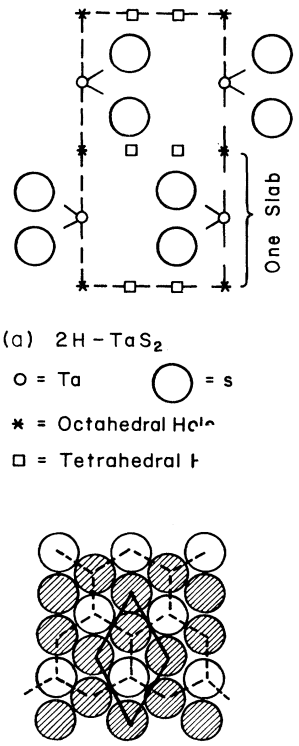

FIG. 1. (a) $(11\bar{2}0)$ plane of the hexagonal $2H$-TaS_2 polymorph. (Taken from Reg. 5.) This is the same structure as $2H$-$NbSe_2$. The positions of the octahedral and tetrahedral holes in the van der Waals gap are indicated. (b) The (0001) projection of the $\frac{2}{3}$-filled octahedral holes.

Å. There are two possible explanations to account for this: First is that the oxidation state of the Tl may be close to three, with a radius of 1 Å, which would be consistent with the observed lattice expansion. The other possibility is that there are structural differences between Tl and the other metals, and that this is reflected in differences in the local symmetry. We were unable to prepare single-phase Ga intercalated $NbSe_2$ and the In intercalated NbS_2 was so highly disordered that little information could be obtained from the diffraction data.

The compositions, routinely determined by weight-gain experiments, varied somewhat but were consistently around $M_{2/3}NbX_2$ for all materials. Figure 1(b) illustrates the (0001) view of this material when $\frac{2}{3}$ of the holes in the van der Waals gap are occupied by the M atoms. This shows an ordered intercalate arrangement of lattice constant $a_0\sqrt{3}$, which should produce a superlattice line in the x-ray diffraction patterns. Since such a line was not observed in our x-ray spectra, this suggests that the structure of intercalates may be disordered. Since no detailed composition vs temperature or composition vs metal vapor pressure studies were done, we are not certain that these are the only "phase(s)" found in the metal intercalated niobium dichalcogenide systems. It should also be mentioned that the intercalation compounds of niobium are considerably different from their tantalum analogs, both in structure and in composition.

The change in the superconducting transition temperature of our samples upon intercalation was determined by measuring the ac susceptibility using a low-frequency mutual-inductance apparatus. None of the intercalated materials was found to superconduct at 1.5 K or above, although the NbS_2 and $NbSe_2$ are superconductors with transition temperatures 6 and 7 K, respectively.

NMR measurements

The properties of both the intercalate and the Nb NMR have been studied from 5 to 20 MHz at temperatures from 1.5 to 4.2 K using both continuous-wave (cw) and pulsed-NMR techniques. The powder samples (325 mesh) were kept under helium atmosphere, and they were checked periodically for deterioration by running the NMR spectrum. We did not see any sign of deterioration in these samples either with time or from recycling them from room temperature to 4.2 K. Our NMR results on the intercalates will be discussed first.

The NMR Knight shift of the ^{205}Tl, ^{119}Sn, and ^{69}Ga intercalates has been measured using the proton resonance as a reference. The In resonance was not observed in either $NbSe_2$ or NbS_2, probably because of its large quadrupole moment. The isotropic Knight shift K_{is} of the intercalates ^{205}Tl, ^{119}Sn, and ^{69}Ga was found to be $(0.21 \pm 0.01)\%$, $(0.24 \pm 0.01)\%$, and $(0.07 \pm 0.01)\%$, respectively. In all cases the intercalate Knight shift was found to be substantially smaller than that of the pure intercalate metal, indicating that the resonance is due to intercalated rather than precipitated metal atoms. Because the intercalate atoms are sitting in a highly anisotropic environment, we might expect a substantial anisotropy in the Knight shift. However, only for the case of Tl have we been able to accurately determine the anisotropy of the Knight shift. The Sn and Pb resonances in the intercalated $NbSe_2$ samples are substantially weaker than those we observed in Sn_xTaS_2 and Pb_xTaS_2 samples with $x = \frac{1}{3}$ or 1. No anisotropic Knight-shift data were obtained for Sn and Pb intercalates in $NbSe_2$. Also no anisotropic Knight-shift data were obtained for the case of Ga since it was difficult to obtain an accurate line shape due to the overlap of the Ga resonance with the broad Nb resonance. The an-

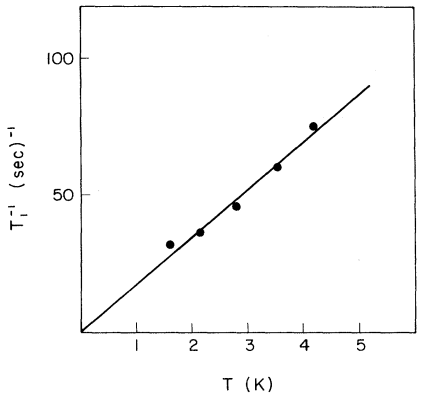

FIG. 2. Relaxation rate, T_1^{-1}, for ^{205}Tl in $Tl_{0.64}NbSe_2$ at 13.00 MHz from 1.5 to 4.2 K.

isotropic Knight shift of Tl, $|\frac{1}{3}(K_{\parallel} - K_{\perp})| = |K_{ax}| = 0.03\%$, was determined from the high-field slope of a plot of the Tl linewidth versus applied magnetic field[12] data. Since an inhomogeneous Knight-shift-broadened resonance line can have the same field dependence of the linewidth, the measured high-field slope determined by such a plot gives an upper limit for the anisotropic Knight shift. Both the isotropic ($K_{1s} = 0.21\%$) and anisotropic ($|K_{ax}| = 0.03\%$) Knight shifts were measured in the temperature range from 1.5 to 4.2 K, and they were found to be temperature independent. These values are found to be smaller than the values[13,14] found in metallic Tl ($K_{1s} = 1.56\%$ and $K_{ax} = 0.082\%$).

Where possible the intercalate spin-lattice relaxation time was measured using a 180°–90° pulse sequence. Only in the case of the Tl intercalated $NbSe_2$ were we able to determine the spin-lattice relaxation time accurately. In the other metal intercalates we could not obtain reliable relaxation-time data either because of the weakness of the resonance or because of overlap with the Nb resonance. The temperature dependence of the Tl spin-lattice relaxation time at 13 MHz is shown in Fig. 2. The recovery of the Tl NMR signal following the 180° pulse was followed for two decades and it was found to be exponential. From Fig. 2 it is clear that T_1T is constant from 1.5 to 4.2 K with $T_1T = 0.0059$ sec K. The linear dependence of the relaxation rate T_1^{-1} on temperature indicates metallic character at the intercalate sites.

From their measurements of the Sn NMR properties of Sn_xTaS_2, where $x = \frac{1}{3}$ or 1, Gossard *et al.*[11] determined that there was metallic character at the intercalate sites, although the spin-lattice relaxation time was found to be impurity dominated and temperature independent in the temperature range from 1.5 to 4.2 K. Our results on the isotropic and anisotropic Knight shift of the Sn resonance in Sn_1TaS_2 are in agreement with those of Gossard *et al.*[11] but we find a temperature-dependent spin-lattice relaxation time of ($T_1T = 0.022$ sec. K) characteristic of metallic behavior. A comparison of the Sn Knight shift in $NbSe_2$ (0.24%) with that in Sn_1TaS_2 (0.78%) and $Sn_{1/3}TaS_2$ (0.08%) suggests that at roughly $\frac{2}{3}$ coverage, the metallic behavior at the Sn site in $NbSe_2$ lies intermediate to the metallic behavior in superconducting Sn_1TaS_2 and the weakly metallic $Sn_{1/3}TaS_2$. As discussed below, this is consistent with the ^{119}Sn Mössbauer results obtained on this sample.

The NMR quadrupole powder pattern of the ^{93}Nb resonance was obtained by integrating the spin echo at constant frequency and sweeping the magnetic field. For a given sample the NMR quadrupole spectrum was obtained at different frequencies from 7 to 15 MHz and at temperatures from 1.5 to 4.2 K. No temperature dependence of the quadrupole spectrum was observed. In the case of $Sn_{2/3}NbSe_2$, two samples were studied and similar spectra were obtained.

The NMR quadrupole spectrum of the Nb resonance from the $Tl_{2/3}NbSe_2$ sample gave the best resolved quadrupole satellites. In Fig. 3(a) we show this spectrum taken at a frequency of 15.5 MHz and at 4.2 K. The two peaks marked as *A* and *B* correspond to the second-order split central

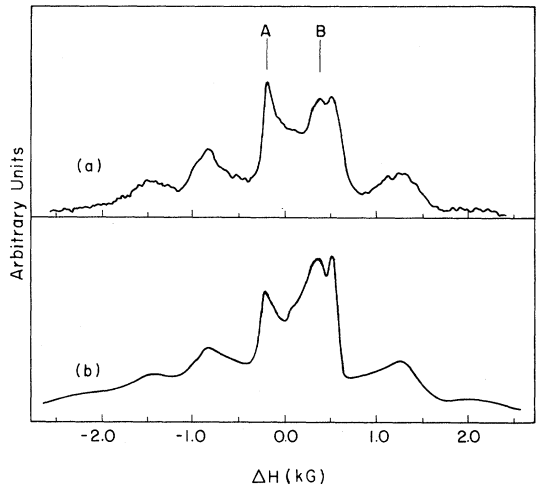

FIG. 3. (a) Experimental NMR quadrupole powder pattern of ^{93}Nb in $Tl_{0.64}NbSe_2$ at 4.2 K. The field at the center of the spectrum is $H_0 = 14.900$ kG. The peaks marked as *A* and *B* arise from the second-order splitting of the central transition. (b) Calculated quadrupole powder pattern assuming axially symmetric field gradients, $\eta = 0$, and an anisotropic Knight shift of $K_{ax} = -0.15\%$. The spectrum is obtained by convolution of the quadrupole powder pattern with two Gaussian broadening functions [see Eq. (1)], one of width αq_0, with $\alpha = 15\%$ describing the EFG distribution and the other of width $\beta = 20$ G representing the Nb resonance linewidth.

transitions, while the peaks on both sides of the central portion correspond to the quadrupole satellites of the spin $I=\frac{9}{2}$ ^{93}Nb nucleus.

In order to compare the observed spectrum with a computer-generated spectrum several factors must be considered. There are two quantities which determine the splitting of the quadrupole satellites, the z component of the EFG, $eq=V_{zz}$, and the asymmetry parameter $\eta=(V_{xx}-V_{yy})/V_{zz}$, where the $V_{ij}(i,\ j=x,y,z)$ are the different components of the field-gradient tensor. For crystal structures which have an n-fold symmetry axis with $n>2$, $\eta=0$ and only one quantity is necessary to determine the quadrupole spectrum. For a given q, and a nonzero η, the first-order correction for the quadrupole interaction will result in shifting the position of the various quadrupole satellites toward the center of the spectrum.[15] In second order, a nonzero η will shift the center of the spectrum toward lower fields[16] by an amount which is proportional to η^2. For $\eta=0$, the distance of the two second-order split central transitions to the center of the spectrum have a ratio[15] of $\frac{9}{16}$. By comparing the experimentally determined quadrupole spectrum in the Tl intercalated $NbSe_2$ sample to calculated spectra, we obtained an upper limit of $\eta=0.07$ for the asymmetry parameter and $(K_{is})_{max}=(0.1\pm0.05)\%$ for the isotropic Nb Knight shift. Since the measured value of η is very small we have calculated the NMR quadrupole powder pattern for all samples assuming $\eta=0$. Both first- and second-order corrections were taken into account for the quadrupole interaction as well as the anisotropic Knight shift. The calculated spectrum shown in Fig. 3(b) is a convolution of the quadrupole powder pattern with two Gaussian broadening functions,

$$G(q-q_0,H-H_0)=\exp[-(q-q_0)^2/(\alpha q_0)^2]\times\exp[-(H-H_0)^2/\beta^2], \quad (1)$$

one of width αq_0 describing the EFG distribution around the average value of q_0 arising from concentration gradients of the intercalate, and the other of width β assuming a Gaussian line shape for the Nb resonance. The good fit of the calculated and experimental Nb NMR spectra for the Tl intercalated $NbSe_2$ sample requires a negative anisotropic Knight shift of $K_{ax}=-0.15\%$ for the Nb resonance.

The Tl intercalated $NbSe_2$ sample was the only one which gave well-resolved peaks for the quadrupole powder pattern and a single q_0 was sufficient to account for all the observed peaks. In all the other samples these peaks are less well resolved and additional peaks were observed which could not be accounted for by a single q_0. A typical line shape is shown for the case of $In_{2/3}NbSe_2$ in Fig. 4(a). It should be noted that none of the peaks shown here can be associated with unintercalated pure $NbSe_2$, because the large EFG in $NbSe_2$ gives much larger splitting of the Nb NMR line. The less well resolved NMR spectra of these samples could arise in several ways. (i) The symmetry of the Nb site could be lowered upon intercalation resulting in asymmetric field gradients, $\eta\neq0$, and a shift of the quadrupole satellites toward the center of the spectrum causing them to overlap. On the basis of the $Tl_{2/3}NbSe_2$ NMR results and the x-ray studies this does not appear to be the case since it would require a large asymmetry parameter to explain the observed smearing of these peaks and would still leave several peaks unaccounted for. (ii) Two inequivalent Nb sites were observed in $2H$-$NbSe_2$ by Ehrenfreund *et al.*[17] at 4.2 K as a result of a lattice distortion at low temperatures. In principle, the existence of two or more inequivalent Nb sites could account for the observed spectra. However, the observed difference in the EFG of the two sites was only about 10%, which is within our values of α. It seems unlikely that a low-temperature lattice distortion of this magnitude can account for the observed spectra. (iii) For the crystal structure of $2H$-$NbSe_2$ there are

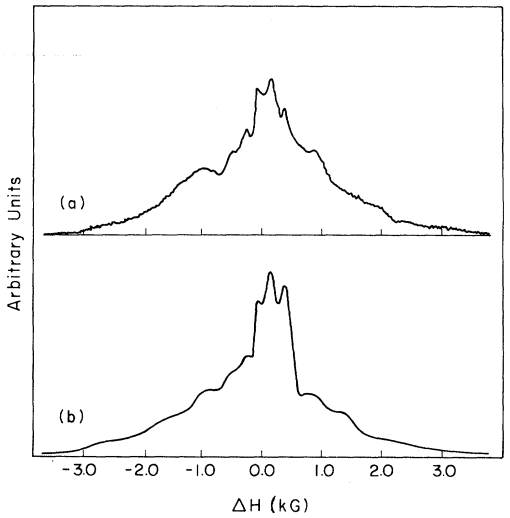

FIG. 4. Experimental NMR quadrupole powder pattern of ^{93}Nb in $In_{0.62}NbSe_2$ at 4.2 K. The field at the center of the spectrum is $H_0=13.487$ kG. (b) Calculated two-site NMR quadrupole powder pattern for axially symmetric field gradients, $\eta=0$. The spectrum represents a superposition of two spectra with a relative isotropic Nb Knight shift of $(K_{is})_1-(K_{is})_2=0.37\%$ and $(K_{ax})_1=(K_{ax})_2=0$. Each spectrum is a convolution of the quadrupole powder pattern with two Gaussian broadening functions [see Eq. (1)], one of width αq_0 which describes the EFG distribution and the other β representing the Nb linewidth. For the first site $\alpha_1=20\%$ and $\beta_1=40$ G. For the second site $\alpha_2=15\%$ and $\beta_2=40$ G.

three possible intercalate sites per Nb atom[5] as shown in Fig. 1(a), two sites with tetrahedral coordination and one site with octahedral coordination. The magnitude of the change in the c-axis lattice parameter for our samples is consistent with intercalate occupation of the octahedral sites. We believe the most likely explanation of the observed NMR spectra is related to the structure of the $x = \frac{2}{3}$ phase[5] shown in Fig. 1. Because of the occupation or nonoccupation of the octahedral sites above and below a given Nb (i.e., in adjacent intercalate layers), three inequivalent Nb sites can result in the $\frac{2}{3}$ phase with probabilities which have ratios of 4:4:1 if the occupation of the octahedral sites is uncorrelated between adjacent layers. If, on the other hand, the intercalate atoms are not confined to a given site, the Nb atoms would sample a large variety of environments. This could result in a large EFG distribution and a complete smearing of the quadrupole satellites.

In order to determine if this last possibility is reasonable, we calculated Nb line shapes assuming a superposition of two equally weighted spectra arising from two inequivalent Nb sites. This, of course, neglects the third inequivalent Nb site. Since this site would contribute only $\frac{1}{9}$ of the total intensity of the NMR line, it would not be possible to determine any parameters on the third site given the large EFG distribution required for the other two sites. In Fig. 4(b) we show a calculated line shape obtained by the superposition of two such Nb spectra, one for an EFG of $q_1 = 3.6$ Å^{-3} with an EFG distribution of 20%, and the other for an EFG of $q_2 = 5.7$ Å^{-3} with an EFG distribution of 15% and [18] $Q(^{93}\mathrm{Nb}) = -0.2$ b. The two site spectra were weighted equally and added assuming a 0.37% difference in the isotropic Knight shift of the two sites. The calculated line shape illustrates the main features of the experimental line shape by reproducing all the peaks and shoulders. The reasonably good fit of the calculated line shape with the experimental one supports the idea that at least two inequivalent sites are required to account for the observed line shape. Although the EFG distribution plays a role in smearing out the quadrupole peaks, it alone cannot account for the observed line shape since we find this is about the same, (15–20)%, for all samples.

Similar fits of the experimental and calculated line shapes from the samples of $NbSe_2$ intercalated with Pb, Sn, and Ga, as well as NbS_2 intercalated with In, were obtained by using the two inequivalent Nb site model. The quadrupole coupling constants, $|e^2qQ/h|$, and the EFG's derived from these computer fits are listed in Table II. For all the intercalated samples we find the EFG at the Nb sites are substantially reduced from those in the unintercalated materials. For the Tl sample the reduction of the EFG from that of pure $NbSe_2$ is about 40%, while in the other samples, where we believe two inequivalent Nb sites can be identified, the reduction of the EFG for one site is about (35–40)% and about 60% for the other site. It is not possible to determine the relation between the intercalate occupation and the EFG at the Nb site, but it would be reasonable to assume that the greatest reduction of the EFG occurs when the octahedral sites above and below a Nb site are occupied by an intercalate and a lesser EFG reduction would occur when only one of these octahedral sites was occupied. The amount of the reduction of the EFG in these samples shows little dependence on the position of the intercalate in the Periodic Table. However, differences in the EFG reductions for the various intercalates clearly exist indicating that the changes occurring in these materials upon intercalation are not independent of the intercalate.

One of the most interesting features of the re-

TABLE II. Measured quadrupolar coupling constants $|e^2qQ/h|$ at 4.2 K for ^{93}Nb in intercalated NbS_2 and $NbSe_2$ compounds of the formula M_xNbX_2 where $x \approx \frac{2}{3}$. $|q|$ and $|\Delta q|$, the change in $|q|$ from the unintercalated compounds, are obtained by assuming $Q(^{93}\mathrm{Nb}) = -0.2$ b (Ref. 18). Numbers in parentheses indicate the estimated uncertainties in the preceding digit.

Material	$\lvert e^2qQ/h\rvert$ (MHz) Site I	Site II	$\lvert q\rvert$ (Å^{-3}) Site I	Site II	$\lvert \Delta q\rvert$ (Å^{-3}) Site I	Site II
$NbSe_2$	62(2)[a]		8.9(3)		...	
NbS_2	60(1)[b]		8.6(2)		...	
$Tl_{0.64}NbSe_2$		37(1)		5.3(2)		3.6(3)
$In_{0.62}NbSe_2$	25(2)	40(3)	3.6(3)	5.7(4)	5.3(4)	3.2(5)
$Pb_{0.63}NbSe_2$	23(2)	35(3)	3.3(3)	5.0(4)	5.6(4)	3.9(5)
$Sn_{0.56}NbSe_2$	23(2)	40(3)	3.3(3)	5.7(4)	5.6(4)	3.2(5)
$Ga_{0.5-0.7}NbSe_2$	Smeared spectrum but with over-all width similar to the other samples					
$In_{0.68}NbS_2$	24(2)	37(3)	3.4(3)	5.3(4)	5.2(4)	3.3(5)

[a]Reference 17. [b]Reference 19.

sults presented in Table II is the difference between the Nb spectra for the Tl and other samples. As discussed earlier, the intercalation of Tl into $NbSe_2$ causes a smaller increase in the c-axis lattice parameter than do the other intercalates. At present the reason for this difference it not well understood since the NMR results show no indication of sample deterioration over a period of several months as well as a symmetric EFG at the Nb site.

In Table II we also list the quadrupole coupling constant for the nonintercalated $NbSe_2$ and NbS_2.[17,19] The value of 62 MHz listed for the case of NbS_2 represents an average value for the two inequivalent sites observed at low temperature.[17]

Mössbauer results

The sample of $Sn_{0.56}NbS_2$ was studied at room temperature using the ^{119}Sn Mössbauer effect. The resulting absorption was well fit by a single line with an isomer shift of 1.06 mm/sec relative to β-tin. (However, the resonance linewidth was broader than observed in β-tin which could indicate a small unresolved quardupole splitting.) As pointed out by DiSalvo *et al.*[5] isomer shifts in this range are consistent with a divalent Sn state. By way of comparison, in Sn_1TaS_2, DiSalvo *et al.*[5] observed a large quadrupole splitting and an isomer shift of 0.50 mm/sec., while in $Sn_{1/3}TaS_2$ only a single resonance was observed with an isomer shift of 1.23 mm/sec. The value of the Sn isomer shift in $NbSe_2$ was found to be between the values observed for the Sn isomer shifts in Sn_xTaS_2 for $x = \frac{1}{3}$ and 1, but closer to that of $x = \frac{1}{3}$. It was for the value $x = \frac{1}{3}$ that the Sn NMR properties[5] in Sn_xTaS_2 indicate weakly metallic character at the intercalate site. No superconductivity was observed[5] above 0.5 K for $x = \frac{1}{3}$. These results of DiSalvo *et al.*[5] are consistent with the observed small Sn Knight shift in $NbSe_2$ and the absence of a superconducting transition above 1.5 K.

DISCUSSION

In order to discuss the Knight shift and spin-lattice relaxation-time data on the intercalate resonances we follow the customary scheme employed for partitioning the bulk susceptibility, Knight shift, and spin-lattice relaxation rate into the s-contact hyperfine contribution and the core polarization and orbital hyperfine contributions from the p and d bands.[20] For the intercalates we have studied, the s-contact hyperfine interaction is expected to dominate the intercalate NMR properties. In terms of the various paramagnetic susceptibility contributions χ_i, and for noninteracting electrons, the Knight-shift terms are given by[20]

$$K_i = (\mu_B N)^{-1} H_{\rm hfs}^{(i)} \chi_i, \tag{2}$$

and the spin-lattice relaxation rates are given by[20]

$$R_i = (T_1 T)_i^{-1} = \frac{4\pi}{\hbar} (\gamma_n \hbar)^2 k_B [H_{\rm hfs}^{(i)} N_i(0)]^2 F_i. \tag{3}$$

The quantities $H_{\rm hfs}^{(i)}$ are the appropriate hyperfine fields (in Oe/μ_B), the N_i (0) are the s-, p-, or d-electron density of states at the Fermi energy (per spin direction), and the F_i are the inhibition factor for the p and d contributions resulting from the orbital degeneracy at the Fermi energy.

For the intercalates studied, the NMR properties should depend primarily on the s and p conduction electrons at the intercalate, although some contribution might arise as a result of transfered hyperfine interactions. Then we can write the relaxation rate as

$$1/T_1 = 1/T_{1s} + 1/T_1', \tag{4}$$

where $(T_1')^{-1}$ represents all non-s electron contributions to the relaxation rate. In the same way we can write the isotropic Knight shift as

$$K_{\rm is} = K_s + K', \tag{5}$$

where K_s is due to the s-contact hyperfine interaction and K' represents all other contributions to the Knight shift. For a given interaction mechanism other than the spin-orbit coupling, a relation of the form[20]

$$K_i^2 T_{1i} T = (k_B \gamma_n^2)^{-1} C_i \tag{6}$$

holds between the Knight shift and the spin-lattice relaxation time, where C_i is a constant characteristic of the interaction mechanism.

For noninteracting s conduction electrons this relation, known as the Korringa relation,[21] becomes

$$K_s^2 T_{1s} T/S = 1, \tag{7}$$

where $S = \mu_B^2/\pi k_B \hbar \gamma_n^2$. For the p-electron core polarization contribution this relation becomes,[20,22]

$$K_{\rm cp}^2 T_{1\,\rm cp} T/S = 3. \tag{8}$$

The temperature dependence of the Tl relaxation rate in $Tl_{0.64}NbSe_2$ [Fig. (2)] indicates the existence of a conduction band at the Tl sites. Both the Tl relaxation rate and isotropic Knight shift are much smaller than observed in metallic Tl,[13,14] indicating a small density of states at the intercalate sites. The Korringa product of $K_{\rm is}^2 T_1 T/S = 0.33$ for the intercalate is substantially smaller than unity, and also smaller than that of metallic Tl by a ratio of $(K_{\rm is}^2 T_1 T)_{\rm int}/(K_{\rm is}^2 T_1 T)_{\rm met} = 0.46$. The small density of states at the Tl site inferred from the NMR data indicates that the deviation from the Korringa product will most probably result from non-s-electron contributions rather than electron-electron interactions. In order to

estimate the various contributions to the Tl NMR properties we assume that the observed spin-lattice relaxation rate is due to the s-contact hyperfine interaction. Using the Korringa product [Eq. (7)] we estimate that $K' = -0.16\%$ for the s-electron contribution to the isotropic Tl Knight shift. Using the measured isotropic Knight shift ($K_{is} = 0.21\%$) we estimate that $K' = 0.16\%$ for the value of all non-s-electron contributions to the Knight shift. We expect K' to arise primarily from p-electron core polarization since K' is negative. We can check the validity of this analysis by using the estimated value of K' and the Korringa relation [Eq. (8)] to estimate the size of the p-electron contribution to the Tl relaxation rate. We find that this contribution is only about 6% and can be neglected.

With the above assumption that the s-contact interaction dominates the Tl relaxation rate we find that the s-contact contribution to the Tl relaxation rate is a factor of 25 smaller than observed in metallic Tl[14] and indicates [Eq. (3)] the s-electron density of states at the Fermi energy is only 15% of that of metallic Tl. The presence of p electrons in the conduction band at the intercalate site is also indicated by the observed anisotropic Knight shift of the Tl resonance. On the basis of our Knight-shift and spin-lattice relaxation data of the intercalate resonance, we conclude that upon intercalation of $NbSe_2$ with post-transition-metal atoms, the s and p electrons of the intercalate atom form a band at the intercalate site which overlaps the narrow d-electron conduction band of the layered compound. This qualitative picture about the nature of the conduction electrons at the intercalate site is consistent with the one suggested by DiSalvo *et al.*[5] for TaS_2 intercalated with metal atoms. Since the intercalate contribution to the conduction-band density of states is small, we are going to ignore its effect in the following duscussion.

In order to interpret the origin of the changes in the EFG at the Nb sites, we follow the approach of Ehrenfreund *et al.*,[19] starting with the assumption of of an ionic crystal. The EFG at the Nb sites can be divided into two contributions,

$$eq = eq_{\text{latt}}(1-\gamma_\infty) + eq_{\text{local}}(1-R). \tag{9}$$

The first term is the EFG due to all point charges located at the lattice points and the second term is due to unfilled d-shell electrons at the Nb sites. Here $\gamma_\infty = -15$ is the Sternheimer antishielding factor and $R = 0.1$ is the corresponding shielding factor.[23]

Ehrenfreund *et al.*,[19] using the summation procedure of de Wette[24] for hexagonal lattices, calculated the lattice contribution for the case of NbS_2. From their calculations they find that the lattice contribution is small and arises almost completely from intralayer charges and that the interlayer distance (provided it is greater than 6 Å) does not affect q_{latt}. This is also the case for $NbSe_2$ since the interlayer distance $d = \frac{1}{2}c$ is 6.27 Å. The intralayer lattice constant is 3.48 Å, which is about 5% larger than in NbS_2.

The local contribution to the EFG can be written[15]

$$eq_{\text{local}} = -e\int |\psi(r)|^2[(3\cos^2\theta - 1)/r^3]d^3r, \tag{10}$$

where $\psi(r)$ is the electronic wave function at a distance r from the Nb nucleus. Only the d electrons of the incompletely filled d shell will contribute to the EFG. If there is no overlap between the valence and conduction bands, as indicated by the band-structure calculations by Mattheiss,[25] then we can write the local contribution as[19]

$$eq_{\text{local}} = -\beta_v \langle r^{-3}\rangle n_v - \beta_c \langle r^{-3}\rangle n_c, \tag{11}$$

where $\beta_c = (3\cos^2\theta - 1)$ is the geometrical factor of the field gradients averaged over the valence- (β_v) or the conduction- (β_c) band electron wave functions and $\langle r^{-3}\rangle$ is averaged over the Nb 4d orbitals. n_v and n_c are the number of valence- and conduction-band d electrons per atom, respectively. Each Nb contributes two d- and two s-electrons to form the compounds $NbSe_2$ or NbS_2. If we consider a single layer of $NbSe_2$, two of the five d orbitals have symmetries xz and yz and belong to the irreducible representation E'', and two with symmetries xy and x^2-y^2 and belong to the E' irreducible representation. These orbitals are in the layer and they are the most probable ones to form the covalent bond between the Nb and Se or S atoms. The fifth d orbital, $3z^2 - r^2$, which belongs to A_1 irreducible representation, is perpendicular to the layers and gives the main contribution to the conduction band. The single d electron per Nb atom outside the full valence band occupies half of the conduction band. The values of β for orbitals in the E'', E', and A_1 irreducible representations are $\beta(E'') = \frac{2}{7}$, $\beta(E') = -\frac{4}{7}$, and $\beta(A_1) = \frac{4}{7}$, and in the case of free Nb^{+2} ion[26] $\langle r^{-3}\rangle = 23$ Å^{-3}.

Upon intercalation of $NbSe_2$ and NbS_2 with metal atoms the observed substantial increase in the distance d between the layers will not affect the lattice contribution to the EFG. Also, there is no evidence that the intercalation changes the nearest-neighbor symmetry of the Nb atoms and the observed nearest-neighbor distance change upon intercalation is less than 1%. Under these conditions the observed change in the EFG should arise from the change in the number of d electrons per Nb atom, n_c, in the conduction band. Using Eqs. (9) and (11) and the observed decrease in the field gradients upon intercalation, we estimated the maximum charge transfer to the conduction band of the layered compound. These values are listed in

TABLE III. Charge transfer to the conduction band calculated from the observed reduction in EFG upon intercalation in the $M_{2/3}NbSe_2$ phase.

Material	Δn_1 (electrons/Nb atom) Site I	Site II
$Tl_{0.64}NbSe_2$		0.35
$In_{0.62}NbSe_2$	0.52	0.31
$Pb_{0.63}NbSe_2$	0.54	0.38
$Sn_{0.56}NbSe_2$	0.54	0.31
$In_{0.68}NbS_2$	0.50	0.32

Table III. A value of $\langle r^{-3}\rangle = 20$ Å^{-3} was used to take into account the expansion of 4*d* orbitals in the solid.[19] Charge transfer from the intercalate atom to the conduction band will leave a net charge at the intercalate site. The contribution of this charge to the EFG at the Nb site is negligible and the values of Table III were not corrected for that effect. Comparing our results on the charge transfer which occurs when $NbSe_2$ or NbS_2 is intercalated with post-transition-metal atoms with those on NbS_2 intercalated with the organic molecule pyridine,[19] we conclude that the charge transfer effect is generally larger in the case of the post-transition-metal atoms than in the case of organic molecule intercalates.

Band-structure calculations by Matteiss[25] on 2*H*-$NbSe_2$ indicate a half-filled narrow *d*-electron conduction band with maximum density of states at the Fermi energy. From his results we estimated that a charge transfer of between 0.31 to 0.54 electrons per Nb atom, such as occurs upon the intercalation of Ga, In, Tl, Sn, or Pb in $NbSe_2$, will result in reducing the density of states at the Fermi energy by more than 50%. Ehrenfreund *et al.*[19] also show that charge transfer occurs upon intercalation of NbS_2 with the organic molecule pyridine. A reduction in the density of states of 2*H*-$NbSe_2$ intercalated with the organic molecule ethylenediamine (EDA) was reported by Meyer *et al.*[4] from their specific-heat data. In both cases, (pyridine)$_{1/2}NbS_2$ and (EDA)$_{1/4}NbS_2$, the superconducting transition temperature T_c was found to decrease. In our intercalated materials we find T_c is reduced below 1.5 K. Although such a decrease of T_c is compatible with a reduced density of states resulting from charge transfer to the Nb *d* band, it is difficult to make a more quantitative statement for the relation between the two. Revelli[27] showed that for the case of TaS_2 and TaS_2 intercalated with pyridine, the observed increase in the density of states was substantially less than required to predict the observed increase of the superconducting transition temperature.

CONCLUSIONS

We have studied several of the bulk and microscopic properties of $NbSe_2$ and NbS_2 intercalated with the post-transition-metal atoms Ga, In, Sn, Tl, and Pb. Most of the intercalated M_xNbX_2 materials are single phase with $x \approx \frac{2}{3}$. All samples show a substantial increase in the *c*-axis parameter perpendicular to the layers relative to the NbX_2 compounds but only a very small change in the intralayer lattice parameter. None of the intercalated materials were found to have a superconducting transition down to 1.5 K. NMR studies of the intercalate nuclei on several of these materials indicate that in the $x = \frac{2}{3}$ phase there is metallic behavior at the intercalate site but that the density of states at the intercalate site is much smaller than in the pure intercalate metals. From the quadrupole splitting of the Nb NMR line we have determined the electric field gradient at the Nb site and the amount of charge transfer from the intercalate to the Nb *d*-electron conduction bands. The charge transfer ranges from 0.31 to 0.54 electrons/(Nb atom). Computer fits to the Nb spectrum indicate that for most of the intercalation compounds at least two inequivalent Nb sites exist. This is consistent with the $x = \frac{2}{3}$ intercalation phase. Only a single Sn Mössbauer resonance line was observed in Sn_xNbSe_2. For the Sn intercalation compound, the Sn isomer shift and the Sn Knight shift lie intermediate to the values found for Sn in the Sn_xTaS_2 intercalation compounds,[5] where $x = 1$ or $\frac{1}{3}$. This is consistent with the metallic behavior of the intercalate in the $M_{2/3}NbX_2$ compounds lying intermediate to the metallic behavior in the superconducting Sn_1TaS_2 and the weakly metallic nonsuperconducting $Sn_{1/3}TaS_2$ phases studied by DiSalvo *et al.*[5]

ACKNOWLEDGMENTS

We would like to thank Dr. H. Myron and Dr. D. E. Ellis for several useful discussions relating to this work, and Dr. C. Wiley and Professor L. Schwartz for obtaining the Sn Mössbauer spectrum. We appreciate the assistance of R. A. Figat in the sample preparation.

*Work supported by AFOSR and NSF through the N. U. Materials Research Center.

†Present address: Corporate Research Center, Universal Oil Products Company, Ten UOP Plaza, Des Plaines, Ill. 60016.

[1]J. A. Wilson and A. D. Yoffe, Adv. Phys. 18, 193 (1969).

[2]F. R. Gamble, J. H. Osiecki, M. Cais, R. Pisharody, F. J. DiSalvo, and T. H. Geballe, Science 174, 493 (1971).

[3]F. R. Gamble, J. H. Osiecki, and F. J. DiSalvo, J. Chem. Phys. 55, 3525 (1971).

[4]S. F. Meyer, R. E. Howard, G. R. Stewart, J. V. Acrivos, and T. H. Geballe (unpublished).

[5]F. J. DiSalvo, G. W. Hull, Jr., L. H. Schwartz, J. M. Voorhoeve, and J. V. Waszczak, J. Chem. Phys. 59, 1922 (1973).
[6]J. M. Voorhoeve, Nee Van Den Berg, and M. Robbins, J. Solid State Chem. 1, 134 (1970).
[7]J. M. Voorhoeve–Van Den Berg, J. Less-Common Metals 26, 399 (1972).
[8]J. M. Van Den Berg and P. Cossee, Inorg. Chim. Acta. 2, 143 (1968).
[9]J. Edwards and R. F. Frindt, J. Phys. Chem. Solids 32, 2217 (1971).
[10]F. J. DiSalvo, R. Schwall, T. H. Geballe, F. R. Gamble, and J. H. Osiecki, Phys. Rev. Lett. 27, 310 (1971).
[11]A. C. Gossard, F. J. DiSalvo, and H. Yasuoka, Phys. Rev. B 9, 3965 (1974).
[12]F. Borsa and R. G. Barnes, J. Phys. Chem. Solids 25, 1305 (1964).
[13]N. Bloembergen and T. J. Rowland, Phys. Rev. 97, 1679 (1955).
[14]N. Karnezos and L. B. Welsh (unpublished).
[15]M. H. Cohen and F. Reif, in *Solid State Physics*, edited by F. Seitz and D. Turnbull (Academic, New York, 1957), Vol. 5, p. 360.
[16]G. H. Stauss, J. Chem. Phys. 40, 1988 (1964).
[17]E. Ehrenfreund, A. C. Gossard, F. R. Gamble, and T. H. Geballe, J. Appl. Phys. 42, 1491 (1971).
[18]K. Murakawa, Phys. Rev. 98, 1285 (1955).
[19]E. Ehrenfreund, A. C. Gossard, and F. R. Gamble, Phys. Rev. B 5, 1708 (1972).
[20]See, for example, A. Narath, in *Hyperfine Interactions*, edited by A. J. Freeman and R. B. Frankel (Academic, New York, 1967); and A. Narath (review article), Crit. Rev. Solid State Sci. 3, 1 (1972).
[21]J. Korringa, Physica 16, 601 (1950).
[22]E. M. Dickson, Phys. Rev. 184, 294 (1969).
[23]We used the same values for γ_∞ and R which were used by Ref. 19.
[24]F. W. de Wette, Phys. Rev. 123, 103 (1961).
[25]L. F. Mattheiss, Phys. Rev. B 8, 3719 (1973).
[26]A. J. Freeman and R. E. Watson, in *Magnetism*, edited by G. T. Rado and H. Suhl (Academic, New York, 1965), Vol. II A, p. 291.
[27]J. Revelli, Ph.D. thesis (Stanford University, 1973) (unpublished).